High-resolution biostratigraphy and chemostratigraphy of the Cenomanian stratotype area (Le Mans, France)

Delphine Desmares, Marc Testé, Bérengère Broche, Maxime Tremblin, Silvia Gardin, Loïc Villier, Edwige Masure, Danièle Grosheny, Nicolas Morel, Patrice Raboeuf

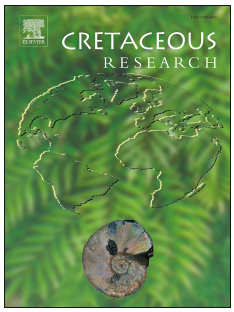

High-resolution biostratigraphy and chemostratigraphy of the Cenomanian stratotype area (Le Mans, France)

Delphine Desmares, Marc Testé, Bérengère Broche, Maxime Tremblin, Silvia Gardin, Loïc Villier, Edwige Masure, Danièle Grosheny, Nicolas Morel, Patrice Raboeuf

PII: S0195-6671(19)30086-2

DOI: https://doi.org/10.1016/j.cretres.2019.104198

Reference: YCRES 104198

To appear in: *Cretaceous Research*

Received Date: 1 March 2019

Revised Date: 12 July 2019

Accepted Date: 31 July 2019

Please cite this article as: Desmares, D., Testé, M., Broche, B., Tremblin, M., Gardin, S., Villier, L., Masure, E., Grosheny, D., Morel, N., Raboeuf, P., High-resolution biostratigraphy and chemostratigraphy of the Cenomanian stratotype area (Le Mans, France), *Cretaceous Research*, https://doi.org/10.1016/j.cretres.2019.104198.

High-resolution biostratigraphy and chemostratigraphy of the Cenomanian stratotype area (Le Mans, France)

Delphine Desmares[a,*], Marc Testé[a, b], Bérengère Broche[a], Maxime Tremblin[c], Silvia Gardin[a], Loïc Villier[a], Edwige Masure[a], Danièle Grosheny[d], Nicolas Morel[e], Patrice Raboeuf[e]

[a] CR2P – Centre de Recherche en Paléontologie – Paris, UMR 7207, Sorbonne Université – MNHN - CNRS, 4, place Jussieu, 75005, Paris, France

[b] Laboratoire de Géographie Physique, 1 Place Aristide Briand, Bâtiment Y, 92195 Meudon sur Seine, France

[c] UMR 7193 ISTeP, Sorbonne Université - CNRS, 4, place Jussieu, 75005, Paris, France

[d] Université de Lorraine - Ecole Nationale Supérieure de Géologie, GéoRessources, UMR7359 - CNRS, 2 Rue du Doyen Marcel Roubault, 54505 Vandoeuvre-lès-Nancy cedex, France

[e] Musée Vert, Muséum d'histoire naturelle du Mans, 204 avenue Jean Jaurès, 72100 Le Mans, France

[*]delphine.desmares@sorbonne-universite.fr

Highlights

- Biostratigraphy and chemostratigraphy of the Cenomanian stratotype area
- Description of *Praeglobotruncana rillella* nov. sp. and of *Dicarinella falsohelvetica* nov. sp.
- Change in coiling direction among *Muricohedbergella delrioensis* during the OAE2

- $\delta^{18}O$ offset between left- and right-coiled *M. delrioensis*

- Correlation between Pueblo (GSSP) and Le Mans area (area of historical type section for the Cenomanian stage)

Abstract

The definition of the Cenomanian stage was based on the description of several type sections scattered in the vicinity of Le Mans (Sarthe, France). Despite limited exposures nowadays, the area remains a reference for the palaeontology of the Cenomanian due to its outstanding richness in marine macrofossils, especially molluscs, bryozoans, brachiopods and echinoderms. The publication in 2015 of the volume dedicated to the Cenomanian stratotype yielded the opportunity to restudy the last accessible outcrops. This paper provides a high-resolution stratigraphic scheme and palaeoenvironmental reconstruction for the middle and late Cenomanian interval in its type area. La Garenne Quarry is a window on the middle Cenomanian, where *Praeglobotruncana rillella* nov. sp. has been identified. The $\delta^{13}C_{carb}$ and $\delta^{18}O_{carb}$ record of a Cenomanian–Turonian succession close to Le Mans is correlated with the type section of Pueblo (Colorado). Isotopic and biotic events highlight the presence of several hiatuses in the sedimentary record of Le Mans especially around the Cenomanian–Turonian boundary with a dramatic truncation of the plateau of high $\delta^{13}C_{carb}$ values. Coiling reversal events among the surface dwellers *Muricohedbergella delrioensis*, indicate sea surface temperature changes with transient coolings, including the *Plenus* cold event, and warm conditions at the Cenomanian–Turonian boundary. Sandy to chalky facies have yielded empty, well-preserved shells of foraminifera allowing the description of *Dicarinella falsohelvetica* nov. sp. Oxygen isotopic analyses performed on right- and left-coiled *M.*

delrioensis reveal a systematic offset during cold events which lead to discuss about the potential occurrence of cryptic species in the Mesozoic.

Keywords Planktonic foraminifera, Middle Cenomanian, Cenomanian–Turonian stage boundary, Oceanic Anoxic Event 2, Anglo-Paris Basin, shell coiling direction

1. Introduction

"*Stratotype Cénomanien*" (Morel, 2015) is a book of the series *Patrimoine géologique* (Geological Heritage) published by the *Muséum national d'Histoire naturelle* of Paris to facilitate access of French historical stratotypes to the scientific community and to a wider audience. The editing of this volume led to the reinvestigation of two historical sections (Saint-Ulphace and Mézières-sur-Ponthouin) close to Le Mans in the Department of Sarthe (Figs. 1, 2, 3).

The Cenomanian stage was originally defined by d'Orbigny in 1847 in his book Paléontologie Française and numerous fossils were collected and described during the 19th century, by d'Orbigny himself as well as by local naturalists such as Guéranger (1850). Most available outcrops around Le Mans became degraded or disappeared at the beginning of the 20th century. Few researchers have reinvestigated the stratigraphy of the Cenomanian type area employing modern standards (Hancock, 1959; Marks, 1967b, a; Juignet, 1973; Juignet et al., 1973; Juignet et al., 1978; Juignet et al., 1983; Ferré, 1995; Robaszynski et al., 1998; Lasseur, 2007; Gaspard, 2014; Gaspard and Loubry, 2017; Kočí et al., 2017). In comparison, hundreds of papers are devoted to the Pueblo GSSP section (Colorado, USA), that encompasses the Cenomanian–Turonian stage boundary. The lack of interest in the historical stratotype area can be explained by the proximal environments it represents and the numerous

erosional surfaces and non-deposition intervals interrupting the sedimentary series. The facies are partly sandy (Fig. 1) and several hardgrounds and erosional surfaces indicate the presence of hiatuses (Juignet, 1973). Another difficulty is that the type Cenomanian cannot be described at one main site but only from a series of sections. Most of the outcrops are now vegetated or urbanized. For example, two of the fourteen formations, which comprise the Cenomanian are no longer accessible (Morel, 2015).

Nevertheless, the stratotype area is a pertinent site, especially because planktonic foraminifera, nannofossil and ammonite biostratigraphic schemes can be coupled with chemostratigraphic analysis. Planktonic foraminifera are particularly well-preserved, although they are quite rare except in the upper Cenomanian – lower Turonian chalky facies. Scanning electron photomicrographs (Figs. 4, 5, 6) show the excellent preservation of detailed surface ornament and test ultrastructure. The test chambers are mostly free of secondary calcite, allowing precise geochemical analyses.

2. Geological setting

Transgressive Albian deposits overlie Jurassic sediments East of Le Mans and Armorican basement to the west (Fig. 1). During the early and middle Cenomanian, the stratotype area was characterized by nearshore sedimentary environments close to Le Mans and by more open marine environments a few tens of kilometres eastwards. Sandy detrital facies alternate with calcareous marls and occasionally chalky deposits; the calcareous formations increasing eastwards of Le Mans (Fig. 1). With the late Cenomanian transgression, chalky facies accumulated through a large part of the Paris Basin (Fig. 1).

La Garenne Quarry at Saint-Ulphace exposes the Sables et Grès de Lamnay and the overlying Craie de Théligny. The site remains one of the last two outcrops of the stratotype

area where the Middle Cenomanian can be accessed (Fig. 2). To conform to regulation, the quarries will be restored to a natural landscape after the end of sand mining (Morel, 2015). The Courgenard borehole, drilled less than three kilometres west of Saint-Ulphace in the 80's, pierced the entire Craie de Théligny and indicates that this formation has a thickness of about twenty metres (Juignet et al., 1983). At La Garenne Quarry, only the basal three metres of the chalky formation are accessible. Above the Théligny hardground, the base of the Craie de Théligny comprises 30 centimetres of a glauconite-rich chalk layer. This basal level contains an abundant fauna of molluscs (bivalves and ammonites). In the Craie de Théligny, ammonites are quite common and diversified; the whole formation is assigned to the middle Cenomanian *Acanthoceras rhotomagense* Zone (Juignet et al., 1978; Morel, 2015).

The Cenomanian–Turonian stage boundary crops out on the banks of the Chemin de la Crêle close to Mézières-sur-Ponthouin village. The section does not present any lithologic evidence (i.e., black shales) of the Oceanic Anoxic Event (OAE2). The section begins in the upper part of the Sables du Perche and ranges up to the Craie à *Inoceramus labiatus* (Fig. 3). However, only about 10 centimetres of the Craie à *I. labiatus* can be sampled in the bank of La Crêle path. The formation is more clearly visible in an outcrop facing the path but estimating how much is missing between the two sites is unclear. As the banks are covered in vegetation, trenches were dug to sample properly the basal part of the section; the chalky facies being the only parts visible on the upper part of the path. Even though this section is one of the most documented ones in the area (Juignet, 1973; Kennedy and Juignet, 1994a; Ferré, 1995; Morel, 2015), it has yielded few ammonites. Most of the ammonites reported from the vicinity of Le Mans have been described from other regional localities. Among rare ammonites collected in Mézières-sur-Ponthouin, *Metoicoceras geslinianum* indicates that the Sables à *Catopygus obtusus* belong to the *M. geslinianum* Zone (Kennedy and Juignet, 1994a). The fauna of the Marnes à *Ostrea biauriculata* in the Sarthe indicates that this

formation belongs to the *Calycoceras guerangeri* Zone (Juignet et al., 1978; Kennedy and Juignet, 1994b; Morel, 2015). According to Kennedy and Juignet (1994a), the basal part of the Craie à *Terebratella carantonensis* can be assigned to the uppermost Cenomanian *Neocardioceras juddii* Zone with one specimen of the nominate species found in Saint-Calais in the eastern part of the Sarthe. In the western part of the Paris Basin, the Turonian is indicated in the Craie à *I. labiatus* by the occurrence of the ammonite *Mammites nodosoides* that is so far not recorded in the stratotype area (Juignet et al., 1973). The Cenomanian–Turonian boundary (CTB) is supposed to be on the upper 2/3 of the Craie à *T. carantonensis* (Juignet, 1973; Robaszynski et al., 1998), a few centimetres below the base of the Craie à *I. labiatus*. The boundary between the two chalky formations is characterized by the disappearance of glauconite.

3. Material and methods

15 samples (with a sampling interval of 20 centimetres) and 40 samples (with a sampling interval varying from 10 to 30 centimetres) were respectively collected at La Garenne Quarry (Fig. 2) and at the Chemin de la Crêle (Fig. 3) for stable isotope analyses and detailed biostratigraphic survey (planktonic foraminifera and nannofossils).

Following standard procedures, sediments were soaked in a peroxide solution and subsequently washed over 63 μm and 1 mm sieves. The planktonic foraminifera have been extracted from this fraction (63 μm-1mm). Particular attention has been given to the *Muricohedbergella delrioensis* population. Due to the low abundance of planktonic foraminifera in the assemblage, only between 50 and 100 specimens of *M. delrioensis* could be counted per sample. Presenting a low trochospiral test with 4.5 to 5.5 globular chambers on the last whorl, the specimens of *M. delrioensis* have been observed from the spiral side.

Right-coiling refers to those specimens that are coiled in a clockwise direction and left-coiling to those that show an anticlockwise coiling. This published work and the nomenclatural acts it contains have been registered in ZooBank. The LSID (Life Science Identifier) for this publication is: urn:lsid:zoobank.org:pub:047E90B9-1CA9-4B02-8165-3865E98AF928. Type and figured specimens of planktonic foraminifera are deposited in the collections of the Sorbonne Université, Paris.

For study of the nannofossil assemblages, 14 samples from La Garenne Quarry at Saint-Ulphace and 30 samples from the Chemin de la Crêle at Mézières were selected and processed in simple smear slides using ammonic distilled water (pH = 8.5). Three traverses of each slide were thoroughly examined using a Zeiss Axioscope imaging at 1500X (cross-polarized and plane light) to locate and quantify key biostratigraphic species. Some samples were also analysed with the SEM in order to check for the preservation state.

Bulk rock carbonate and *M. delrioensis* were analysed for oxygen and carbon stable isotope composition with a Kiel IV mass spectrometer. Organic matter was removed from the carbonates by soaking the sample overnight in 5% sodium hypochlorite solution. For *M. delrioensis* isotope analysis, about 5 to 6 empty individuals were selected, cleaned in an ultrasonic bath and analysed. Stable isotope values were calibrated relative to the Vienna Pee Dee Belemnite (‰VPDB) via the NBS-19 international standard. The reproducibility of measurements is ±0.1‰ for $\delta^{18}O_{carb}$ and ±0.05‰ for $\delta^{13}C_{carb}$. All analytical results are listed in Appendix A.

4. Results

4.1. La Garenne Quarry at Saint-Ulphace

Planktonic foraminifera are abundant in the first centimetres of Craie de Théligny. The basal glauconitic beds yielded only small triserial *Guembelitria cretacea* (Fig. 2). The assemblage becomes more diversified above the glauconitic levels. Almost all the samples of the assemblage contain rare *Rotalipora cushmani* (Figs. 2, 4). Most specimens of this index species are small with 4 to 5.5 chambers on the last whorl (Fig. 4). Some of them present a highly convex spiral side and are close to *Rotalipora cushmani* var. *expansa* described by Carbonnier (1952). Other rotaliporids such as *Thalmanninella brotzeni* and *Thalmanninella globotruncanoides* are rare. *Praeglobotruncana* are particularly abundant and diversified (Figs. 5, 6) with *Praeglobotruncana aumalensis*, *Praeglobotruncana* aff. *oraviensis*, *Praeglobotruncana gibba*, *Praeglobotruncana rillella* Desmares nov. sp., *Praeglobotruncana stephani*, and *Praeglobotruncana* aff. *Dicarinella hagni*. Some medium-sized to large *Praeglobotruncana* with a distinctive lobate periphery and a thick row of pustules (at least at the beginning of the last whorl) are quite similar to *P. oraviensis* (Fig. 5). According to Falzoni et al. (2016) the first occurrence of this species should be close to the Cenomanian–Turonian boundary. Specimens from the middle Cenomanian of Saint-Ulphace present more pustulose tests than the specimens illustrated and described by Falzoni et al. (2016). *P.* aff. *oraviensis* could be considered as earlier occurrences of *P. oraviensis*. However, the presence of specimens morphologically intermediate between *P. aumalensis* and *P.* aff. *oraviensis* raise the question of an eventual test alteration linked to some sort of environmental pressure. Those forms could also be interpreted as transitional forms between *Praeglobotruncana* and first *P.* aff. *D. hagni* (Fig. 5) recorded in the upper part of the section (Fig. 2). *P.* aff. *Dicarinella hagni* present a typical profile of *D. hagni* but have not yet acquired two keels. These morphotypes with a pustulose band were already described by Robaszynski et al. (1993) in the uppermost lower Cenomanian of Central Tunisia.

The globular forms *Whiteinella aprica* and *M. delrioensis* (Fig. 4) are also well-represented. Contrary to the assumption of the Time Scale 2012 (Anthonissen and Ogg, 2012), *W. aprica* cannot be an objective marker of the upper Cenomanian base, as this species is already recorded in the middle Cenomanian.

The percentages of left-coiled morphotypes among *M. delrioensis* are quite high with values ranging between 35% and 55%.

Calcareous nannofossils are relatively common to abundant and moderately to well-preserved in the Saint-Ulphace assemblages. No specific biohorizons (appearance/disappearance) were highlighted through this section, but the common occurrence of *Litraphidites acutus*, *Axopodorhabdus albianus*, *Helenea chiastia*, *Cretharhabdus striatus*, and the absence of *Gartnerago theta*, seems to indicate an age not older than the middle Cenomanian, roughly corresponding to biozones CC10 (Sissingh, 1977; Perch-Nielsen, 1985) UC3 (Burnett, 1998).

The $\delta^{13}C_{carb}$ curve does not present any positive isotopic excursion (Fig. 2); values are relatively constant (comprise between 1‰ and 2‰).

4.2. Mézières-sur-Ponthouin

The lower and middle parts of Marnes à *O. biauriculata* did not yield any calcareous microfossils. The planktonic foraminifera occur first in this formation just below the Bousse hardground within the last 50 centimetres of the Marnes à *O. biauriculata* (Fig. 3). Among them several specimens of the index species *R. cushmani* have been found in association with other keeled forms, including *Thalmanninella greenhornensis* and *Dicarinella hagni*. It should be noticed that maybe related to the shallow-water settings, all the specimens of *Th. greenhornensis* (Fig. 4) are smaller than usual, and they do not exceed 300 μm at Mézières-

sur-Ponthouin. Two morphotypes of *D. hagni* are commonly found, the classical biconvex forms and more planoconvex morphotypes, with a flat spiral side, that were already described and figured in Robaszynski et al. (1979) and in the upper Cenomanian Sables du Perche Formation in the Civray-de-Touraine borehole (Amédro et al., 2018) (Fig. 7). As previously recorded by Ferré (1995), the last specimens of *R. cushmani* were identified just below the Bousse hardground. In the PhD memoir of Ferré (1995), several occurrences of index species *Helvetoglobotruncana helvetica* are mentioned, but not figured, in the Craie à *I. labiatus* one metre above the disappearance of the glauconitic chalk (Fig. 3). But we did not find any specimen of this latter species. However, several vaulted *Dicarinella* occurred within the Craie à *T. carantonensis* (Figs. 3, 4, 7). These morphotypes are similar in shape to *Dicarinella concavata* with their distinctive bowl-shaped profiles but with discrete staircase-like imbricate structures on spiral side (Fig. 7). It was particularly surprising assuming that the lowest record of *D. concavata* was in the Upper Turonian of Tunisia, on the southern Tethyan margin (Robaszynski et al., 1990). These double-keeled planoconvex variants are quite common and have already been observed in the Upper Cenomanian in different paleogeographic domains. In particular, similar forms were also recognized at Hot Springs in the Western Interior Basin (Fig. 7). We considered that this upper Cenomanian form represent a new species *Dicarinella falsohelvetica* Desmares nov. sp. Evolution of similar planoconvex morphotypes could be iterative or could be linked with environmental conditions. The phylogenetic relationships between *D. hagni* planoconvex morphotypes, *Dicarinella falsohelvetica and D. concavata* have yet to be clarified. The lowest occurrence (LO) of *D. concavata* has been considered to be a reliable biomarker for placement of the base of the upper Turonian–lower Coniacian *D. concavata* Zone (Sigal, 1955; Robaszynski et al., 1990; Premoli Silva and Sliter, 1995; Robaszynski and Caron, 1995) but several studies have already illustrated the diachronous nature of this marker (Robaszynski et al., 1990; Petrizzo, 2000).

The chalky facies in the upper part of the Mézières-sur-Ponthouin section contain abundant and well-preserved nannofossils while in the lower part assemblages are sparse and sediments often barren. A succession of key nannofossil biohorizons, (disappearances of *C. striatus, L. acutus, A. albianus, H. chiastia* and appearance of *Quadrum intermedium, Eprolithus octopetalus*, *E. moratus, Q. gartneri*) has been recorded at Mézières-sur-Ponthouin (Figs. 3, 8) which constrains the CTB interval (Fig. 3), in agreement with published literature (Tsikos et al., 2004; Desmares et al., 2007; Fernando et al., 2010; Linnert et al., 2011; Corbett et al., 2014) and the planktonic foraminifera data.

Whiteinella and *Muricohedbergella* are common and well-represented at Mézières-sur-Ponthouin. The population of *M. delrioensis* exhibits major changes from the Marnes à *O. biauriculata* to the Craie à *T. carantonensis* formations. In the last 50 centimetres of the Marnes à *O. biauriculata*, the percentage of the left-coiled morphotype (Fig. 9) drops significantly from 36% to 16%. Above the Bousse hardground, the percentage of sinistral specimens is again greater than 20%. In the Sables à *C. obtusus*, a general progressive decrease of the number of left-coiled morphotype is observed, and only right-coiled forms are present at the base of the Craie à *T. carantonensis*. In the glauconitic chalk, the percentages of sinistral forms increase again but never exceed 15%.

Due to the outcrop conditions and to the low carbonate percentage, only two values of $\delta^{13}C_{carb}$ were acquired in the Marnes à *O. biauriculata* (Fig. 9). The Sables à *C. obtusus* are characterized by strong $\delta^{13}C$ values (greater than 3,5 ‰) in its lower half (Fig. 9) and by lighter values on its upper half (between 0 and 1‰). The Craie à *T. carantonensis* exhibits a single moderate peak of $\delta^{13}C$ values (Fig. 9).

$\delta^{18}O_{carb}$ presents heavier values above the Bousse hardground in the basal part of the Sables à *C. obtusus* before a change to lighter values in the upper part of the formation (Fig.

9). The values remain within the same range up to the basal part of the Craie à *I. labiatus*. $\delta^{18}O$ performed on dextral and sinistral *M. delrioensis* follow a similar overall trend (Fig. 10).

5. Discussion

5.1. Stratigraphic framework

The Mid-Cenomanian Event I is defined by double $\delta^{13}C_{carb}$ peaks (Ia and Ib) within the middle Cenomanian (Jenkyns et al., 1994; Paul et al., 1994). In the English Chalk, high-resolution chemostratigraphy integrated with ammonite biostratigraphy (Paul et al., 1994; Mitchell et al., 1996; Jarvis et al., 2006) indicated that the two positive $\delta^{13}C_{carb}$ excursions Ia and Ib respectively occur in the *Cunningtoniceras inerme* Zone and in the lower part of the *A. rhotomagense* Zone. If the *C. inerme* Zone is not represented in the north-eastern part of Sarthe (Morel, 2015), we have investigated the possibility of recording Ib in the basal part of the Craie de Théligny. However, the $\delta^{13}C_{carb}$ curve does not present any noticeable variation (Fig. 2). As previously reported in the Courgenard borehole (Juignet et al., 1983), data on planktonic foraminifera indicated that the basal part of the Craie de Théligny in Saint-Ulphace area already belongs to the *R. cushmani* total range Zone that begins in the middle Cenomanian and extends upwards to the Upper Cenomanian in the Anglo-Paris Basin, an age which is also confirmed by nannofossil assemblages. In England, the first *R. cushmani* appears just after a sharp increase in the proportion of planktonic foraminifera: the Planktonic/Benthic event (P/B event). Rotaliporidae become a significant element of the planktonic assemblage in the Anglo-Paris Basin after the P/B event (Paul et al., 1994; Jarvis et al., 2006). In the Théligny area, due to the facies change between the Sables and Grès de Lamnay and the Craie de Théligny, the recognition of a P/B event is not possible. However,

as observed by Juignet et al. (1983), Rotaliporidae are already common in the first metres of the Craie de Théligny. Close to the P/B break, isotopic $\delta^{13}C_{carb}$ values are quite low and stable even if on longer time series (Jarvis et al., 2006), the P/B break corresponds to an inflection point to more rapidly rising $\delta^{13}C_{carb}$ values. Such a trend is not visible in La Garenne Quarry. Considering the ammonite biostratigraphic data, foraminiferal assemblages and the stable low $\delta^{13}C_{carb}$ values, it can be assumed that the basal part of the Craie de Théligny is post Mid-Cenomanian Event I and coeval with the P/B event. Consequently, the base of the *A. rhotomagense* Zone is probably not recorded in the Théligny area suggesting a hiatus. It is in accordance with the presence of an often phosphatised macrofauna at the base of the Craie de Théligny indicating low sedimentation rate and reworking.

The Cenomanian–Turonian stage boundary coincided worldwide with an increase in marine productivity and with the burial of organic carbon (Jenkyns, 1980). Consequently, OAE2 is characterised by a major $\delta^{13}C_{carb}$ positive excursion (Fig. 9). This isotopic shift, composed of high frequency events, is synchronous and allows high-resolution correlations between distant sites (Tsikos et al., 2004; Kuhnt et al., 2005; Grosheny et al., 2006; Desmares et al., 2007; Takashima et al., 2009; Westermann et al., 2010). The initial increase of the $\delta^{13}C_{carb}$ and peak of values (A) is particularly well recorded at Mézières-sur-Ponthouin in the sandy facies above the Bousse hardground. By contrast, the second increase and plateau (B) within the Craie à *T. carantonensis* appears to be particularly reduced (Fig. 9). This weak expression could be related to presence of one or several hiatuses. Juignet (1973) characterised an erosional surface between the Sables à *C. obtusus* and the Craie à *T. carantonensis.*

The extension of this (these) hiatus(es) needs to be constrained with an integrative stratigraphic approach. As surface dwellers, muricohedbergellids were not affected by OAE2

and provide a continuous signal throughout the Cenomanian–Turonian boundary interval (Desmares et al., 2016). Several reversals in coiling direction have been characterised in mid-latitude sections of the Western Interior Seaway and of the Umbria-Marche and Vocontian basins (Desmares et al., 2016; Grosheny et al., 2016). The recognition of these events at Mézières-sur-Ponthouin provides stratigraphic markers.

5.2. Coiling reversal events among *M. delrioensis*

Among some modern and recent fossil species of planktonic foraminifera, the proportion of left- to right-coiled shells in a population appears to be temperature-dependent; the relative abundance of each morphotype reflecting ecological preferences (Ericson, 1959; Bandy, 1960; Boltovskoy, 1973; Bauch et al., 2003; Darling et al., 2006; Darling and Wade, 2008; Ujiie et al., 2010). A similar relationship has been identified among *M. delrioensis* at the Cenomanian–Turonian stage boundary in several mid-latitude sites (Desmares et al., 2016; Grosheny et al., 2016), including the Pueblo type section (Fig. 9). As an example, at Pueblo, the increase of left-coiled *M. delrioensis* in the assemblage is clearly related to higher $\delta^{18}O_{carb}$ values suggesting that changes in the coiling direction in this surface dweller represent a new proxy for constraining Sea Surface Temperature (SST) variations (Desmares et al., 2016; Grosheny et al., 2016). At Pueblo, several events were previously identified in the pattern of *M. delrioensis* shell coiling (Fig. 9):

(S1) An important rise in the relative percentage of sinistral *M. delrioensis* begins in the upper part of the *Metoicoceras mosbyense* Zone. Associated with heaver $\delta^{18}O_{carb}$ values, this event indicates a cooling episode (Desmares et al., 2016). S1 persists into the lower part of the *Sciponoceras gracile* Zone (*M. geslinianum* equivalent) before a stepwise decline. A brief

drop subdivides this event into two episodes: S1a and S1b. Temporally, the base of S1b is coincident with the first peak (A) of the $\delta^{13}C_{carb}$ curve.

(S2) Of lesser amplitude, S2 occurs in the upper part of the *S. gracile* Zone and pertains to the general progressive decrease in frequency of sinistral forms. The end of S2, at the base of the *N. juddii* Zone, coincides with the onset of the $\delta^{13}C_{carb}$ plateau of values (B) and with the beginning of the *Heterohelix* shift (Leckie et al., 1998; Caron et al., 2006; Desmares et al., 2007)

(D) Close to the CTB, right-coiled *M. delrioensis* become dominant. This event is coeval with the $\delta^{13}C_{carb}$ plateau of values (B). In accordance with $\delta^{18}O_{carb}$ values, the dominance of right-coiling forms records a thermal maximum.

Based on the ammonite biostratigraphy and $\delta^{13}C_{carb}$ excursions, most of the events among *M. delrioensis* can be recognized at Mézières-sur-Ponthouin (Fig. 9).

The high proportion of sinistral forms recorded in the upper part of the Marnes à *O. biauriculata* can correspond to the base of S1. However, as the contact between the Sables à *C. obtusus* and the Marnes à *O. biauriculata* is erosive, it cannot be excluded that this sinistral event records an earlier cooling event (Fig. 9). Indeed, new data from the Hartland Shale in the Pueblo section indicated other major coiling reversals within the *M. mosbyense* Zone (Fig. 9).

The high abundance of sinistral morphotypes above the Bousse hardground, coeval with the first peak (A) of $\delta^{13}C_{carb}$ pertains to the S1b event. As for the Pueblo section, S1b is associated with heavier $\delta^{18}O_{carb}$ values and thus clearly reflects a cooling event. This cooling episode is particularly well-expressed in southern England where the positive $\delta^{18}O_{carb}$ excursion (Jarvis et al., 2011) within the mid-*M. geslinianum* Zone is recognizable and coincides with the *Plenus* Cold Event, a temporary influx of Boreal fauna throughout Europe (Jefferies, 1962; Gale and Christensen, 1996). However, at Mézières-sur-Ponthouin, the

373 percentage of sinistral *M. delrioensis* during S1 is significantly lower (Fig. 9). Such a
374 discrepancy could indicate higher SST in the Anglo-Paris Basin even if the two reference
375 sites, historical stratotype and GSSP, are both located within an epicontinental seaway at a
376 similar palaeolatitude of about 40°N (Torsvik et al., 2012; van Hinsbergen et al., 2015).

377 With very few left-coiled specimens, the D event is clearly identified within the basal
378 part of the Craie à *T. carantonensis*. In more detail, in Pueblo, the D event exhibits three
379 successive lows; the first one, the lowest, belonging to the *N. juddii* Zone. In accordance with
380 the ammonite biostratigraphy (Kennedy and Juignet, 1994a), the low records at Mézières-sur-
381 Ponthouin could correspond to the first low of Pueblo. Then, the progressive increase of
382 sinistral forms could be correlated to the same trend observed in the lower Turonian of
383 Pueblo, coeval with the end of the $\delta^{13}C_{carb}$ plateau of values.

384 S2 seems to be incompletely recorded but the boundary between the Sables à *C.*
385 *obtusus* and the Craie à *T. carantonensis* corresponds to an erosion surface (Juignet, 1973).
386 This incomplete pattern can therefore be explained by a hiatus that includes the onset of the
387 $\delta^{13}C_{carb}$ plateau of values (B).

388

389 5.3. Significance of the $\delta^{18}O$ offset between dextral and sinistral morphotypes of *M.*
390 *delrioensis*

391

392 When sinistral *M. delrioensis* exceeds a threshold of 12%, a significant isotopic
393 difference of at least 0.5‰ (up to 1.3‰) between left-coiled *M. delrioensis* and right-coiled
394 *M. delrioensis* is observed (Fig. 10); dextral *M. delrioensis* being systematically lighter and
395 presumably warmer. Such results are particularly surprising because they are similar to what
396 has been published for the *Neogloboquadrina pachyderma* isotopic signature (Bauch et al.,
397 2003; Nyland et al., 2006). An isotopic difference of about 0.5‰ has been highlighted

between left- and right-coiling *N. pachyderma*, since 10 Ka (Bauch et al., 2003). Recent advances in molecular analysis provide new insights concerning the diversity of planktonic foraminifera which has been underestimated while focusing only on the morphological features of the test (Bauch et al., 2003; Darling et al., 2006; Darling and Wade, 2008); morphospecies as previously understood, being in fact composed of several cryptic species. Among the extant *N. pachyderma* s.l., the dextral forms now named *Neogloboquadrina incompta* and the left-coiled *N. pachyderma*. They are in fact different species with distinct ecologies and biogeographic distributions (Darling et al., 2006). Thus, the Holocene $\delta^{18}O$ offset between left-coiled *N. pachyderma* and right-coiled *N. incompta* may 1) represent a genotype-specific vital effect (Bauch et al., 2003) or 2) be related to hydrological factors such as different calcification depths (Bauch et al., 2003; Nyland et al., 2006). Similar assumptions might arise for the *M. delrioensis* population. Does the systematic $\delta^{18}O$ difference reflect a vital effect and/or correspond to any hydrological factor?

Genetic evidence (Bauch et al., 2003; Darling et al., 2006) among *N. pachyderma* s.l. show that the morphological distinction of coiling directions is not sufficient to distinguish two morphotypes; low level (<3%) of aberrant coiling being associated with both morphotypes (Bauch et al., 2003). As an example, a small percentage of tests with a right coiling morphology (1–3%) are found in planktonic assemblages and persist in the sedimentary record even in the most extreme polar conditions. Despite their right coiling morphology, such forms have a sinistral isotopic composition (Bauch et al., 2003). Similarly, it could be argued that during the latest Cenomanian warming and the early Turonian thermal maximum, the rare left-coiled *M. delrioensis* are aberrant forms of the right-coiled variety. It could explain why in this interval, sinistral *M. delrioensis* and dextral *M. delrioensis* have a similar isotopic signature. Interestingly, while the $\delta^{18}O$ reveals a systematic offset, there is no marked difference in $\delta^{13}C$ either between sinistral *N. pachyderma* and dextral *N. incompta*

(Bauch et al., 2003) neither between sinistral *M. delrioensis* and dextral *M. delrioensis* over the entire time interval (Fig. 10). Since $\delta^{13}C$ values of foraminifers are thought to record specific environmental conditions, the similar $\delta^{13}C$ signatures between sinistral and dextral forms could mean that the $\delta^{18}O$ offset represents a genotype-specific vital effect rather than reflecting hydrological factors. As an example, Wang (2000) and Numberger et al. (2009) showed that different $\delta^{13}C$ values in distinct morphotypes of *Globigerinoides ruber* reflect their depth habitat within the water column. Regardless, such a conclusion must be taken with caution as the $\delta^{13}C$ of left-coiled *N. pachyderma* is about constant with water depth (Bauch et al., 2002) meaning that the influence of $\delta^{13}C$ of the dissolved inorganic carbon in the foraminiferal shell can be masked by other effects.

In conclusion, as for sinistral *N. pachyderma* and dextral *N. incompta*, it remains difficult to determine whether the coiling-dependent $\delta^{18}O$ offset among *M. delrioensis* represents annual, seasonal or water-depth hydrological differences rather than a vital effect signature.

6. Systematic Palaeontology

Order FORAMINIFERIDA Eichwald, 1830

Suborder GLOBIGERININA Delage and Hérouard, 1896

Family HEDBERGELLIDAE Loeblich & Tappan, 1961

Genus *Dicarinella* Porthault, 1970

Dicarinella falsohelvetica Desmares, nov. sp.

LSID urn:lsid:zoobank.org:act:7C728E33-B64C-4A03-A1AF-1FE5FDE95C20

Description. Typical forms included in this species have a large (> 400 μm) planoconvex test with 5 to 6 chambers on the final whorl. Equatorial periphery is lobate. On the spiral side, chambers are petaloid in shape and present a discrete staircase-like imbricated chamber. The species presents a bowl-shaped profile with two well-expressed keels. Its umbilicus is narrow. Umbilical sutures are radial and depressed.

Remarks. This species is distinguished from *H. helvetica* by having two keels. It differs from *Dicarinella marianosi* by its smaller size, a fewer number of chambers on the last whorl and its narrower umbilicus. The spiral side of *D. falsohelvetica* is less depressed than *D. concavata.*

Test size. Maximum test diameter: holotype 430 μm, illustrated paratypes 450 μm-500 μm.

Type locality. Chemin de la Crêle, Mézières sur Ponthouin, Cenomanian stratotype area (Sarthe, France).

Type horizon. Cenomanian-Turonian stage boundary, Craie à *Carantonensis* Fm.

Repository. Holotype (collection number MEZ Craie 1, P6M4365, Fig. 7, 5a-c) and paratypes (collection numbers P6M4364, P6M4366, P6M4367, P6M4368, Fig. 7., 4a-c, 6a-b, 7a-b 8a-b) are deposited in the collections of the Sorbonne Université, Paris, France.

Derivation of the name. Due to the shape of its lateral view, this species could be misidentified as a specimen of *H. helvetica* but with two keels.

Genus *Praeglobotruncana* Bermudez, 1952

Praeglobotruncana rillella Desmares, nov. sp.

LSID urn:lsid:zoobank.org:act:D8BAB6CC-27CB-4CC1-874F-0FA2F9F28FBD

Description. Typical forms included in this species have a large (> 350 μm) planoconvex test with 5 to 6 chambers on the final whorl. Equatorial periphery is lobate. On the spiral side, chambers are petaloid in shape and have a coarsely porous aspect, at least on the last whorl, whereas in the inner whorl, porosity is partly hidden by large pustules. Sutures on the spiral side are curved and slightly raised except between the last chambers where it becomes depressed. This species is seemingly "double-keeled" but in detail it presents umbilical well-developed pustules but the last chamber is entirely smooth. On the umbilical side, sutures are radial and depressed; chambers are inflated and triangular in shape. Principal aperture is umbilical and is protected by a narrow lip. The species presents a prominent nonporous carinal band composed of numerous pustules in the earlier part of the last whorl. This band can be less distinct on the final chamber. Even if this species was not abundant enough in the samples to realise a representative count, both dextral and sinistral forms have been found.

Remarks. This species is distinguished from *Whiteinella praehelvetica* (Trujillo, 1960) by a quadratic edge on the last chambers, by a non-pustulose test on the spiral side of the last chamber, by slowly expanding chambers and by a pustulose carinal band in the earlier part of the last whorl. Moreover, 95% of *W. praehelvetica* are dextral forms whereas *P. rillella* exhibits both dextral and sinistral morphotypes. This species differs from the Turonian

497 species *Helvetoglobotruncana microhelvetica* Huber and Petrizzo, 2017 by its larger size and
498 the absence of keel.
499
500 Test size. Maximum test diameter: holotype 370 μm, illustrated paratype 480 μm; maximum
501 breadth: holotype 300 μm, illustrated paratype 400 μm.
502
503 Type locality. La Garenne Quarry at Saint-Ulphace, Cenomanian stratotype area (Sarthe,
504 France).
505
506 Type horizon. Middle Cenomanian (*A. rhotomagense* Zone and *R. cuhmani* Zone), Craie de
507 Théligny Fm., within the three metres above the contact between the formations of “Sables
508 and Grès de Lamnay” and “Craie de Théligny”.
509
510 Repository. Holotype (collection number UP15, P6M4360, Fig. 6, 3a-c) and paratypes
511 (collection numbers UP15, P6M4358, P6M4359, Figs. 1a-c, 2a-c) are deposited in the
512 collections of the Sorbonne Université, Paris, France.
513
514 Derivation of the name. Derived from the Middle French: "rillé" (piece of pork) and dedicated
515 to the local "pâté" of Le Mans area.
516
517 7. Conclusions
518
519 Samples of middle Cenomanian from Saint-Ulphace yield diverse and well-preserved
520 planktonic foraminifera assigned to the *R. cushmani* Zone in accordance with nannofossil
521 data. Among planktonic foraminifera, *Praeglobotruncana* are particularly well-represented.

Their excellent preservation allows the description of a new species *P. rillella* and the opening of discussion on some transitional morphotypes between *Praeglobotruncana* and *Dicarinella*.

At Mézières-sur-Ponthouin, several biohorizons among nannofossils and planktonic foraminifera are identified including the disappearance of *T. greenhornensis* and *R. cushmani* below the Bousse hardground. Sinistral event S1b is recognised in the lower part of the Sable à *C. obtusus*. Bio- and chemostratigraphic correlations with the type section of Pueblo highlight the presence of small hiatuses in the stratotype area. While the first peak (A) of $\delta^{13}C$ values is clearly recognized in the sandy facies above the Bousse hardground, the plateau (B) is limited to the Craie à *T. carantonensis*. This plateau is coeval with the Dextral event (D) encompassing the CTB at Pueblo. In the almost complete absence of specimens of ammonite in this section, this integrated stratigraphic study supports the regional age calibration of the series proposed from ammonite biozonation and suggests that CTB is placed in the middle part of the condensed Craie à *T. carantonensis.*

Acknowledgments

The authors thank Nathalie Labourdette for running the mass spectrometer, Alexandre Lethiers for the drawings. The authors acknowledge funding of the ASM Patrimoine (Muséum national d'Histoire naturelle, Paris). Martin Pickford is thanked for checking the English. The authors wish to emphasize the contributions of Francis Robaszynski to this work with numerous discussions and helpful comments. The authors are especially grateful to Eduardo Koutsoukos and Mark Leckie whose corrections and suggestions improved this manuscript significantly. The authors also thank the anonymous reviewer.

547

548 References

549

550 Amédro, F., Matrion, B., Robaszynski, F., 2018. Stratotype Turonien. Publications
551 scientifiques du Muséum national d'Histoire naturelle & Editions Biotope, 414 p p.
552 Anthonissen, D.E., Ogg, J.G., 2012. Appendix 3: Cenozoic and Cretaceous
553 Biochronology of Planktonic Foraminifera and Calcareous Nannofossils, in: Gradstein, F.M.,
554 Ogg, J.G., Schmitz, M.D., Ogg, G.M. (Eds.), The Geologic Time Scale. Elsevier, pp. 1083-
555 1127.
556 Bandy, O.L., 1960. The geologic significance of coiling ratios in the foraminifer
557 *Globigerina pachyderma*. Journal of Paleontology 34, 671-681.
558 Bauch, D., Darling, K., Simstich, J., Bauch, H.A., Erlenkeuser, H., Kroon, D., 2003.
559 Palaeoceanographic implications of genetic variation in living North Atlantic
560 *Neogloboquadrina pachyderma*. Nature 424, 299-302.
561 Bauch, D., Erlenkeuser, H., Winckler, G., Pavlova, G., Thiede, J., 2002. Carbon
562 isotopes and habitat of polar planktic foraminifera in the Okhotsk Sea: the 'carbonate ion
563 effect' under natural conditions. Marine Micropaleontology 45, 83-99.
564 Boltovskoy, E., 1973. Note on the determination of absolute surface water
565 paleotemperature by means of the foraminifer *Globigerina bulloides* d'Orbigny.
566 Paläontologische Zeitschrift 47, 152-155.
567 Burnett, J.A., 1998. Upper Cretaceous, in: Bown, P.R. (Ed.), Calcareous Nannofossil
568 Biostratigraphy. Chapman and Hall/ Kluwer Academic Publishers, London, pp. 132–199.
569 Carbonnier, A., 1952. Sur un gisement de Foraminifères d'âge cénomanien supérieur
570 provenant de la région de Toza (Maroc). Bulletin de la Société Géologique de France 2, 111-
571 122.
572 Caron, M., Dall'Agnolo, S., Accarie, H., Barrera, E., Kauffman, E.G., Amedro, F.,
573 Robaszynski, F., 2006. High-resolution stratigraphy of the Cenomanian/Turonian boundary
574 interval at Pueblo (USA) and Wadi Bahloul (Tunisia): stable isotope and bio-events
575 correlation. Geobios 39, 171-200.
576 Corbett, M.J., Watkins, D.K., Pospichal, J.J., 2014. Calcareous nannofossil
577 paleoecology of the mid-Cretaceous Western Interior Seaway and evidence of oligotrophic
578 surface waters during OAE2. Marine Micropaleontology 109, 30-45.

Darling, K., Kucera, M., Kroon, D., Wade, C.M., 2006. A resolution for the coiling direction paradox in *Neogloboquadrina pachyderma*. Paleoceanography 21, PA2011.

Darling, K.F., Wade, C.M., 2008. The genetic diversity of planktonic foraminifera and the global distribution of ribosomal RNA genotypes. Marine Micropaleontology 67, 216-238.

Desmares, D., Crognier, N., Bardin, J., Testé, M., Beaudoin, B., Grosheny, D., 2016. A new proxy for Cretaceous paleoceanographic and paleoclimatic reconstructions: Coiling direction changes in the planktonic foraminifera *Muricohedbergella delrioensis*. Palaeogeography, Palaeoclimatology, Palaeoecology 445, 8-17.

Desmares, D., Grosheny, D., Beaudoin, B., Gardin, S., Gauthier-Lafaye, F., 2007. High resolution stratigraphic record constrained by volcanic ash beds at the Cenomanian-Turonian boundary in the Western Interior Basin, USA. Cretaceous Research 28, 561-582.

Ericson, D.B., 1959. Coiling Direction of *Globigerina pachyderma* as a Climatic Index. Science 130, 219-220.

Falzoni, F., Petrizzo, M.R., Jenkyns, H.C., Gale, A.S., Tsikos, H., 2016. Planktonic foraminiferal biostratigraphy and assemblage composition across the Cenomanian–Turonian boundary interval at Clot Chevalier (Vocontian Basin, SE France). Cretaceous Research 59, 69-97.

Fernando, A.G.S., Takashima, R., Nishi, H., Giraud, F., Okada, H., 2010. Calcareous nannofossil biostratigraphy of the Thomel Level (OAE2) in the Lambruisse section, Vocotian Basin, southeast France. Geobios 43, 45–57.

Ferré, B., 1995. Incidences des événements anoxiques océaniques sur les microfaunes cénomano-turoniennes du Bassin anglo-parisien. Université Pierre et Marie Curie, Paris, p. 447.

Gale, A.S., Christensen, W.K., 1996. Occurence of the belemnite *Actinocamax plenus* in the Cenomanian of SE France and its signifiance. Bulletin of the Geological Society of Denmark 43, 68-76.

Gaspard, D., 2014. Noteworthy brachiopods of the Cenomanian stratotype: A synthesis of the biochronological, palaeoenvironmental and palaeoecological implications. Geobios 47, 347-370.

Gaspard, D., Loubry, P., 2017. A brachiopod shell show during the middle Cenomanian in the stratotype area (France) – exceptional residual colour pattern. Annales de Paléontologie 103, 81-85.

Grosheny, D., Beaudoin, B., Morel, L., Desmares, D., 2006. High-resolution biostratigraphy and chemostratigraphy of the Cenomanian-Turonian event in the Vocontian Basin, southeast France. Cretaceous Research 27, 629-640.

Grosheny, D., Ferry, S., Lécuyer, C., Thomas, A., Desmares, D., 2016. The Cenomanian-Turonian Boundary Event (CTBE) on the southern slope of the Subalpine Basin (SE France) and its bearing on a probable tectonic pulse on a larger scale. Cretaceous Research 72, 39-65.

Guéranger, E., 1850. Etude paléontologique sur la stratigraphie du Terrain Cénomanien des environs du Mans. Bulletin de la Société géologique de France 2, 800–807.

Hancock, J.M., 1959. Les ammonites du Cénomanien de la Sarthe, Colloque sur le Crétacé supérieur français. Comptes Rendus du 84e Congrès des Sociétés savantes, Dijon, pp. 249–252.

Jarvis, I., Gale, A.S., Jenkyns, H.C., Pearce, M., 2006. Secular variation in Late Cretaceous carbon isotopes: a new d13C carbonate reference curve for the Cenomanian-Campanian (99.3-70.6). Geological magazine 143, 561-608.

Jarvis, I., Lignum, J.S., Gröcke, D.R., Jenkyns, H.C., Pearce, M.A., 2011. Black shale deposition, atmospheric CO2 drawdown, and cooling during the Cenomanian□Turonian Oceanic Anoxic Event. Paleoceanography 26.

Jefferies, R.P.S., 1962. The palaeoecology of the *Actinocamax plenus* subzone (lowest Turonian) in the Anglo□Paris Basin. Palaeontology 4, 609–647.

Jenkyns, H.C., 1980. Cretaceous anoxic events : from continents to oceans. Journal of the Geological Society, London 137, 171-188.

Jenkyns, H.C., Gale, A.S., Corfield, R.M., 1994. Carbon- and oxygen-isotope stratigraphy of the English Chalk and Italian Scaglia and its palaeoclimatic significance. Geological magazine 131, 1-34.

Juignet, P., 1973. La transgression crétacée sur la bordure orientale du Massif Armoricain. Aptien, Albien, Cénomanien de Normandie et du Maine. Le stratotype du Cénomanien. Université de Caen, p. 806.

Juignet, P., Damotte, R., Fauconnier, D., Kennedy, W.J., Magniez-Janin, F., Monciardini, C., Odin, G.S., 1983. Etude de trois sondages dans la région-type du Cénomanien. La limite Albien-Cénomanien dans la Sarthe (France). Géologie de la France 3, 193-234.

Juignet, P., Kennedy, W.J., 1976. Faunes d'ammonites et biostratigraphie comparée du Cénomanien du nord-ouest de la France (Normandie) et du Sud de l'Angleterre. Bulletin

trimestriel de la Société géologique de Normandie et des Amis du Muséum du Havre 63, 1-193.

Juignet, P., Kennedy, W.J., Lebert, A., 1978. Le Cénomanien du Maine : formations sédimentaires et faunes d'ammonites du stratotype. Géologie méditerranéenne V, 87-100.

Juignet, P., Kennedy, W.J., Wright, C.W., 1973. La limite Cénomanien-Turonien dans la région du Mans (Sarthe) : Stratigraphie et Paléontologie. Annales de Paléontologie 59, 209-242.

Kennedy, W.J., Juignet, P., 1994a. A revision of the ammonite faunas of the type Cenomanian 6. Acanthoceratinae (*Calycoceras* (*Proeucalycoceras*), *Eucalycoceras*, *Pseudocalycoceras*, *Neocardioceras*), Euomphaloceratinae, Mammitinae and Vascoceratidae. Cretaceous Research 15, 469-501.

Kennedy, W.J., Juignet, P., 1994b. A revision of the ammonite faunas of the type Cenomanian, 5. Acanthoceratinae *Calycocera*s (*Calycoceras*), *C.* (*Gentoniceras*) and *C.* (*Newboldiceras*). Cretaceous Research 15, 7-57.

Kočí, T., Jäger, M., Morel, N., 2017. Sabellid and serpulid worm tubes (Polychaeta, Canalipalpata, Sabellida) from the historical stratotype of the Cenomanian (Late Cretaceous; Le Mans region, Sarthe, France). Annales de Paléontologie 103, 45-80.

Kuhnt, W., Luderer, F., Nederbragt, A., Thurow, J., Wagner, T., 2005. Orbital-scale record of the late Cenomanian–Turonian oceanic anoxicevent (OAE-2) in the Tarfaya Basin (Morocco). International Journal of Earth Sciences 94, 147-159.

Lasseur, E., 2007. La craie du Bassin de Paris (Cénomanien-Campanien, Crétacé supérieur) Sédimentologie de faciès, stratigraphie séquentielle et géométrie 3D. Université de Rennes 1, p. 409.

Leckie, R.M., Yuretich, R.F., West, O.L.O., Finkelstein, D., Schmidt, M.G., 1998. Paleoceanography of the southwestern Western Interior Sea during the time of the Cenomanian-Turonian boundary (Late Cretaceous), in: Arthur, M.A., Dean, W.E. (Eds.), Stratigraphy and paleoenvironments of the Cretaceous Western Interior seaway. SEPM Concepts in Sedimentology and Paleontology, pp. 101-126.

Linnert, C., Mutterlose, J., Mortimore, R., 2011. Calcareous nannofossils from Eastbourne (Southeastern England) and the paleoceanography of the Cenomanian–Turonian boundary interval. Palaios 26, 298–313.

Marks, P., 1967a. Foraminifera from the Craie de Théligny (Cénomanien, dépt. Sarthe, France). Proceedings of the Koninklijke Nederlandse Akademie van Wetenschappen 70, 425-442.

Marks, P., 1967b. *Rotalipora* et *Globotruncana* dans la Craie de Théligny (Cénomanien, dépt de la Sarthe). Proceedings of the Koninklijke Nederlandse Akademie van Wetenschappen 70, 264-275.

Mitchell, S.F., Paul, C.R.C., Gale, A.S., 1996. Carbon isotopes and sequence stratigraphy, in: Howell, J.A., Aitken, J.F. (Eds.), High Resolution Sequence Stratigraphy: Innovations and Applications. Geological Society of London, Special Publication, pp. 11-24.

Morel, N., 2015. Stratotype Cénomanien. Publications scientifiques du Muséum national d'Histoire naturelle & Editions Biotope.

Numberger, L., Hemleben, C., Hoffmann, R., Mackensen, A., Schulz, H., Wunderlich, J.-M., Kucera, M., 2009. Habitats, abundance patterns and isotopic signals of morphotypes of the planktonic foraminifer *Globigerinoides ruber* (d'Orbigny) in the eastern Mediterranean Sea since the Marine Isotopic Stage 12. Marine Micropaleontology 73, 90-104.

Nyland, B.F., Jansen, E., Elderfield, H., Andersson, C., 2006. *Neogloboquadrina pachyderma* (dex. and sin.) Mg/Ca and d18O records from the Norwegian Sea. Geochemistry Geophysics Geosystems 10, 18p.

Paul, C.R.C., Mitchell, S.F., Marshall, J.D., Leary, P.N., Gale, A.S., Duane, A.M., Ditchfield, P.W., 1994. Palaeoceanographic events in the Middle Cenomanian of Northwest Europe. Cretaceous Research 15, 707-738.

Perch-Nielsen, K., 1985. Mesozoic calcareous nannofossils, in: Bolli, H.M., Saunders, J.B., Perch-Nielsen, K. (Eds.), Plankton Stratigraphy. Cambridge University Press, pp. 329-426.

Petrizzo, M.R., 2000. Upper Turonian–lower Campanian planktonic foraminifera from southern mid–high latitudes (Exmouth Plateau, NW Australia): biostratigraphy and taxonomic notes. Cretaceous Research 21, 479-505.

Premoli Silva, I., Sliter, W.V., 1995. Cretaceous planktonic foraminiferal biostratigraphy and evolutionary trends from the Bottaccione section, Gubbio, Italy. Palaeontographia Italica 82, 1-89.

Robaszynski, F., Caron, M., 1995. Foraminifères planctoniques du Crétacé : commentaire de la zonation europe-méditerranée. Bulletin de la Société Géologique de France 166, 681-692.

Robaszynski, F., Caron, M., Amédro, F., Dupuis, C., Hardenbol, J., González-Donoso, J.M., Linares, D., Gartner, S., 1993. Le Cénomanien de la région de Kalaat Senan (Tunisie centrale) : litho-biostratigraphie et interprétation séquentielle. Revue de micropaléontologie 12, 351-505.

Robaszynski, F., Caron, M., Dupuis, C., Amédro, F., González Donoso, J.M., Linares, D., Hardenbol, J., Gartner, S., Calandra, F., Deloffre, R., 1990. A tentative integrated stratigraphy in the Turonian of central Tunisia: formations, zones and sequential stratigraphy in the Kalaat Senan area. Bull. Centres Rech. Explor.-Prod. Elf-Aquitaine 14, 213-384.

Robaszynski, F., Caron, M., planctoniques, g.d.t.e.d.f., 1979. Atlas des foraminifères planctoniques du Crétacé moyen (mer boréale et Téthys). Cahiers de Micropaléontologie 1. pp 185. 2. pp 181.

Robaszynski, F., Gale, A.S., Juignet, P., Amédro, F., Hardenbol, J., 1998. Sequence stratigraphy in the Upper Cretaceous series of the Anglo-Paris Basin: exemplified by the Cenomanian stage, in: Graciansky, P.-C., Hardenbol, J., Jacquin, T., Vail, P.R. (Eds.), Mesozoic and Cenozoic Sequence Stratigraphy of European Basins. SEPM, pp. 363-386.

Sigal, J., 1955. Notes micropaléontologiques nord-africaines. 1. Du Cénomanien au Santonien : zones et limites en faciès pélagiques. Compte rendu sommaire des séances de la Société géologique de France 8, 157-160.

Sissingh, W., 1977. Biostratigraphy of Cretaceous calcareous nannoplankton. Geologie en Mijnbouw 56, 37-65.

Takashima, R., Nishi, H., Hayashi, K., Okada, H., Kawahata, H., Yamanaka, T., Fernando, A.G., Mampuku, M., 2009. Litho-, bio- and chemostratigraphy across the Cenomanian/Turonian boundary (OAE 2) in the Vocontian Basin of southeastern France. Palaeogeography, Palaeoclimatology, Palaeoecology 273, 61-74.

Torsvik, T.H., van der Voo, R., Preeden, U., Mac Niocaill, C., Steinberger, B., Doubrovine, P., van Hinsbergen, D.J.J., Domeier, M., Gaina, C., Tohver, E., Meert, J., McCausland, P.J.A., Cocks, L.R.M., 2012. Phanerozoic polar wander, palaeogeography and dynamics. Earth-Science Reviews 114, 325-368.

Tsikos, H., Jenkyns, H.C., Walsworth-Bell, B., Petrizzo, M.-R., Forster, A., Kolonic, S., Erba, E., Premoli Silva, I., Baas, M., Wagner, T., Sinninghe Damste, J.S., 2004. Carbon-isotope stratigraphy recorded by the Cenomanian-Turonian Oceanic Anoxic Event: correlation and implications based on three key localities. Journal of Geological Society 161, 711-719.

Ujiie, Y., De Garidel-Thoron, T., Watanabe, S., Wiebe, P., De Vargas, C., 2010. Coiling dimorphism within a genetic type of the planktonic foraminifer *Globorotalia truncatulinoides*. Marine Micropaleontology 77, 145-153.

van Hinsbergen, D.J.J., de Groot, L.V., van Schaik, S.J., Spakman, W., Bijl, P.K., Sluijs, A., Langereis, C.G., Brinkhuis, H., 2015. A Paleolatitude Calculator for Paleoclimate Studies. Plos one, 21p.

Wang, L., 2000. Isotopic signals in two morphotypes of *Globigerinoides ruber* (white) from the South China Sea: implications for monsoon climate change during the last glacial cycle. Palaeogeography, Palaeoclimatology, Palaeoecology 361, 381-394.

Westermann, S., Caron, M., Fiet, N., Fleitmann, D., Matera, V., Adatte, T., Föllmi, K., 2010. Evidence for oxic conditions during oceanic anoxic event 2 in the northern Tethyan pelagic realm. Cretaceous Research 31, 500-514.

Figure Captions

Figure 1. A. Palaeogeographic setting of the Anglo-Paris Basin, modified after Juignet and Kennedy (1976). B. Lithostratigraphy of the Cenomanian stratotype area with the location of Mézières-sur-Ponthouin and Saint-Ulphace, modified after Juignet et al. (1978).

Figure 2. Distribution of planktonic foraminifera in the basal part of the Craie de Théligny Fm. at La Garenne Quarry (Saint-Ulphace) set against $\delta^{13}C_{carb}$ and $\delta^{18}O_{carb}$.

Figure 3. Distribution of planktonic nannofossils at the Chemin de la Crêle (Mézières-sur-Ponthouin). The base of the *H. helvetica* Zone is placed after Ferré (1995).

Figure 4. 1a-c. *Rotalipora cushmani* (Morrow, 1934), UP15, P6M4339. 2a-c. *R. cushmani*, MEZ10, P6M4340. 3a-c. *Thalmanninella globotruncanoides* (Sigal, 1948), UP18, P6M4341. 4a-c. *R. cushmani* var. *expansa*, UP15, P6M4342. 5a-b. *Thalmanninella brotzeni* Sigal, 1948, UP18, P6M4343. 6a-b. *Thalmanninella greenhornensis* (Morrow, 1934), MEZ11, P6M4344.

7a-c. *Whiteinella aprica* (Loeblich and Tappan, 1961), MEZ Craie 1, P6M4345. 8a-b. *Globigerinelloides bentonensis* (Morrow, 1934), MEZ10, P6M4346. 9a-c. *Muricohedbergella delrioensis* (Carsey, 1926), MEZ Craie 1, P6M4347. 10a-c. *W. aprica* (Loeblich and Tappan, 1961), UP15, P6M4348. 11a-c. *M. delrioensis*, UP15, P6M4349.

Figure 5. 1a-c. *Praeglobotruncana aumalensis* (Sigal, 1952), UP15, P6M4350. 2a-c. *P. aumalensis*, UP15, P6M4351. 3a-c. *Praeglobotruncana stephani* (Gandolfi, 1942), UP12, P6M4352. 4a-c. *P. stephani*, UP12, P6M4353. 5a-c. *Praeglobotruncana gibba* (Klaus, 1942), UP18, P6M4354. 6a-c. *Praeglobotruncana* sp. aff. *Dicarinella hagni* (Scheibnerova, 1962), UP15, P6M4355. 7a-c. Intermediate between *P. aumalensis* and *Praeglobotruncana* aff. *oraviensis* Scheibnerova 1960, UP15, P6M4356. 8a-c. *Praeglobotruncana* aff. *oraviensis*, UP15, P6M4357.

Figure 6. 1a-c, 2a-c. *Praeglobotruncana rillella*, n. sp., paratype, UP15, P6M4358, P6M4359. 3a-c. *Praeglobotruncana rillella*, n. sp., holotype, UP15, P6M4360.

Figure 7. 1a-c. *D. hagni*, biconvex morphotype, MEZ Craie 1, P6M4361. 2a-c. *D. hagni*, intermediate morphotype between planoconvex and biconvex forms, MEZ Craie 1, P6M4362. 3a-c. *D. hagni*, planoconvex morphotype, Civray (France), upper Cenomanian (Turonian stratotypic area), P6M4363. 4a-c. *Dicarinella falsohelvetica* n. sp., paratype, MEZ Craie 1, P6M4364. 5a-c. *D. falsohelvetica* n. sp., holotype, MEZ Craie 1, P6M4365. 6a-b. *D. falsohelvetica* n. sp., paratype, MEZ Craie 1, P6M4366. 7a-b., 8a-c. *D. falsohelvetica* n. sp., paratype, HS9, Hot Springs (South-Dakota, US), upper Cenomanian (*S. gracile* Zone), P6M4367, P6M4368.

Figure 8. 1. *Cretarhabdus striatus* (Stradner 1963) Black, 1973; sample MEZ 12. 2. *Eiffellithus* cf *E. eximius* (Stover, 1966) Perch-Nielsen 1968; sample MEZ 29. 3. *Axopodorhabdus albianus* (Black, 1967) Wind & Wise *in* Wise & Wind, 1977; sample MEZ 12. 4. *Eprolithus octopetalus* Varol, 1992; sample MEZ 34. *Eprolithus moratus* (Stover, 1966) Burnett, 1998; sample MEZ 39. *Gartnerago segmentatum* (Stradner, 1966) Thierstein, 1974; sample MEZ 12. 7. *Quadrum intermedium* Varol, 1992; sample MEZ 28. 8. *Quadrum gartneri* Prins and Perch-Nielsen 1977; sample MEZ 37. 9. *Lithraphidites acutus* Verbeek & Manivit, 1977; sample MEZ 12. Scale bar = 5μm.

Figure 9. $\delta^{18}O_{carb}$ and $\delta^{13}C_{carb}$ records compared to the changes in the percentage of sinistral *M. delrioensis* in the sections at Pueblo (Desmares et al., 2016) and at Mézières-sur-Ponthouin. Isotopic $\delta^{13}C$ events A: initial increase in values and first peak; B: second increase and plateau.

Figure 10. Carbon and oxygen isotopic compositions for left-coiled (white dots) and right-coiled *M. delrioensis* (black dots) at Mézières-sur-Ponthouin. Data are compared with bulk isotopic composition and with the percentage of sinistral morphotypes.

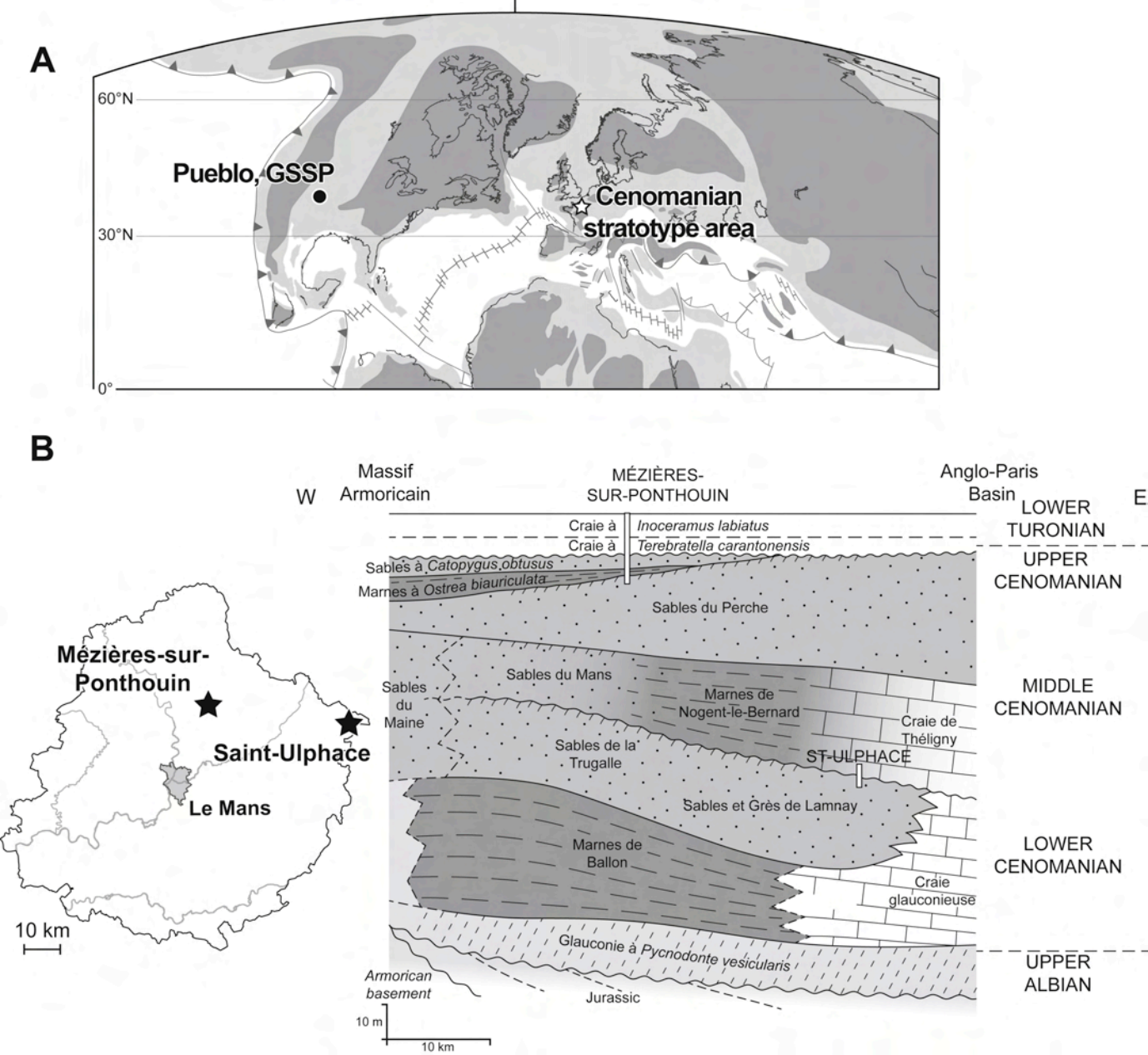
A
60°N
30°N
0°
Pueblo, GSSP
Cenomanian
stratotype area
B
W
Massif
Armoricain
MÉZIÈRES-
SUR-PONTHOUIN
Anglo-Paris
Basin
E
LOWER
TURONIAN
UPPER
CENOMANIAN
MIDDLE
CENOMANIAN
LOWER
CENOMANIAN
UPPER
ALBIAN
Craie à Inoceramus labiatus
Craie à Terebratella carantonensis
Sables à Catopygus obtusus
Marnes à Ostrea biauriculata
Sables du Perche
Sables du Mans
Sables
du
Maine
Marnes de
Nogent-le-Bernard
Craie de
Théligny
ST-ULPHACE
Sables de la
Trugalle
Sables et Grès de Lamnay
Marnes de
Ballon
Craie
glauconieuse
Glauconie à Pycnodonte vesicularis
Armorican
basement
Jurassic
10 m
10 km
Mézières-sur-
Ponthouin
Saint-Ulphace
Le Mans
10 km

Saint-Ulphace
La Garenne Quarry

Mézières-sur-Ponthouin

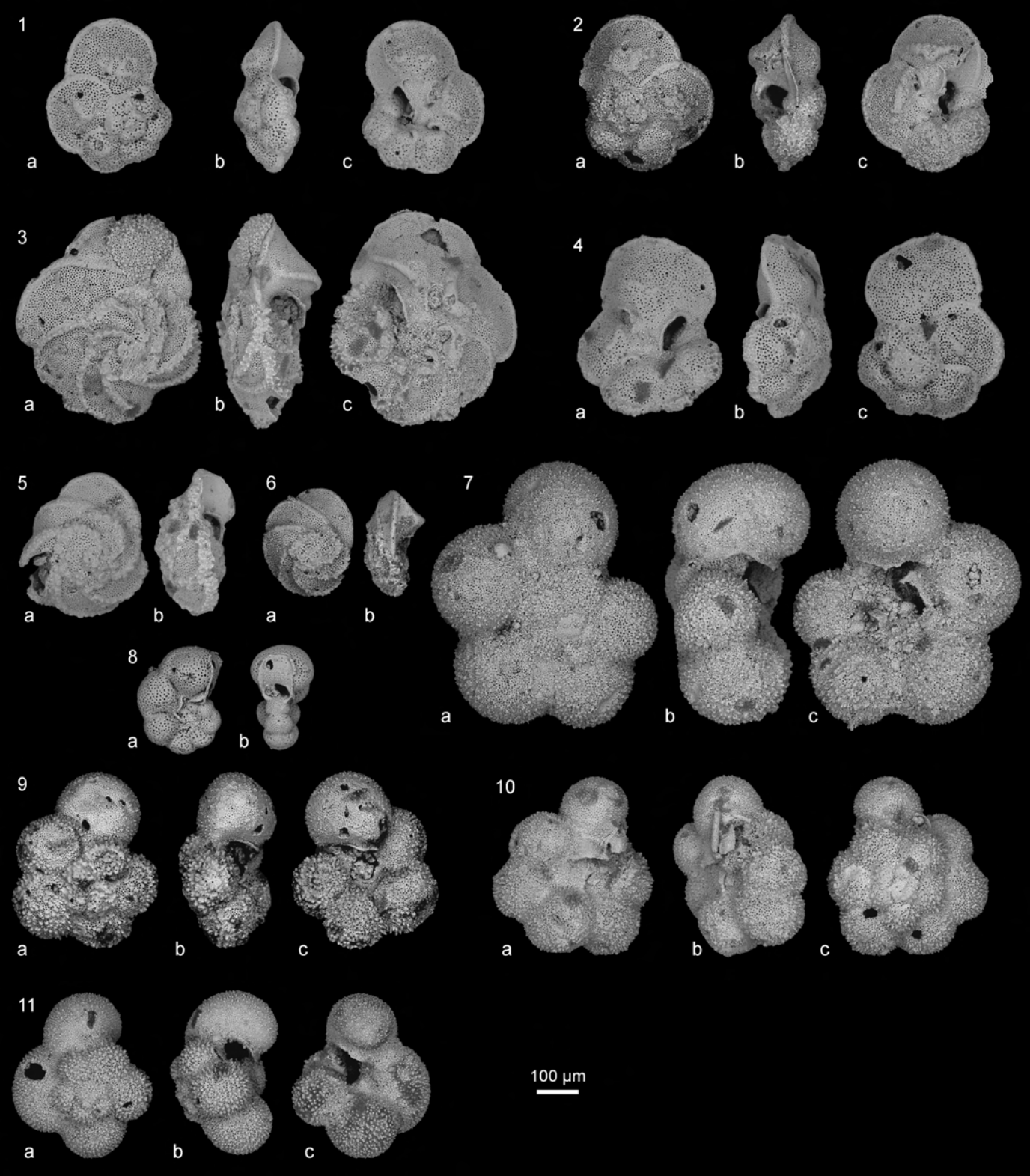
1
a
b
c
2
a
b
c
3
a
b
c
4
a
b
c
5
a
b
6
a
b
7
a
b
c
8
a
b
9
a
b
c
10
a
b
c
11
a
b
c
100 µm

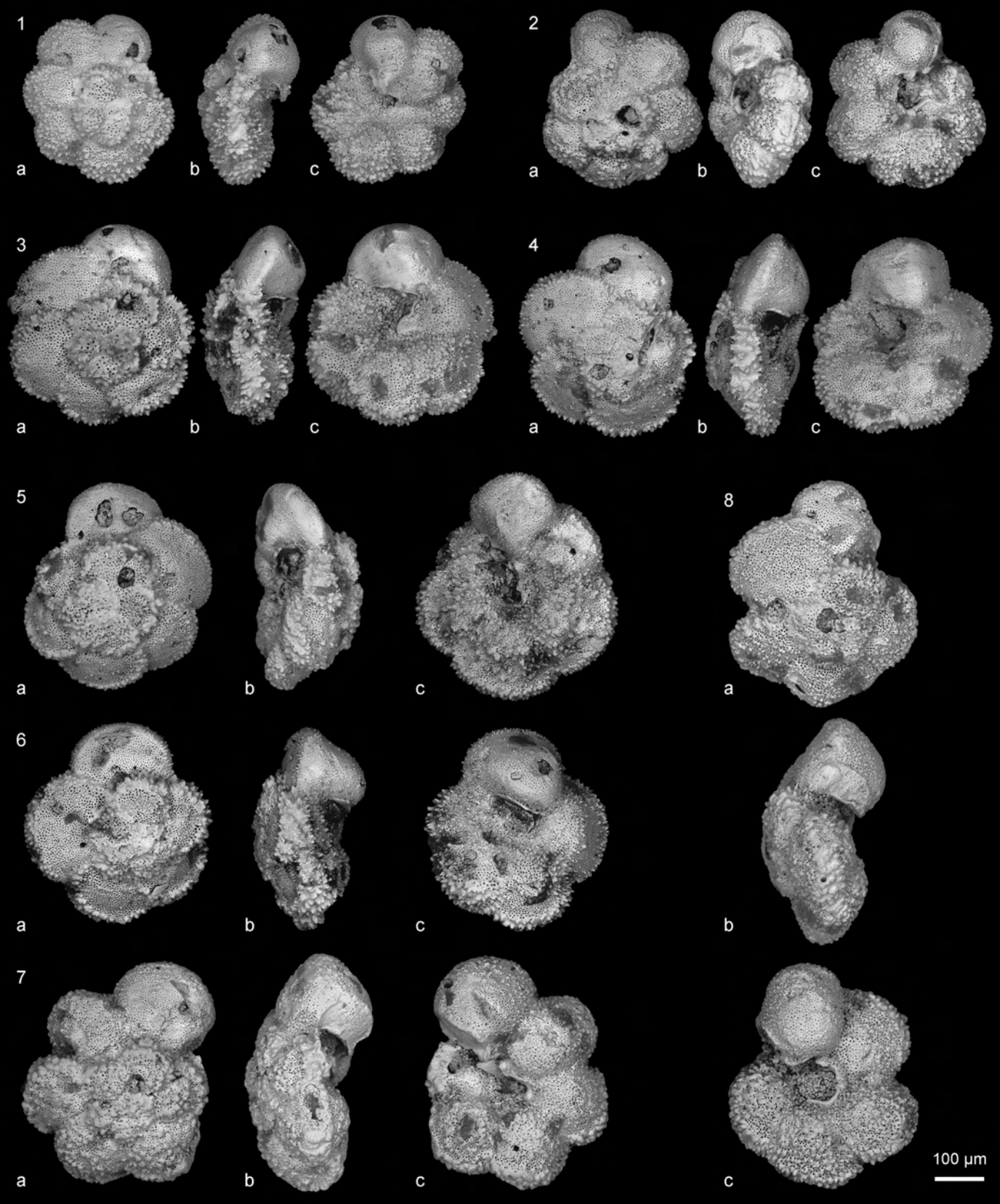
1
a
b
c
2
a
b
c
3
a
b
c
4
a
b
c
5
a
b
c
8
a
6
a
b
c
b
7
a
b
c
c
100 µm

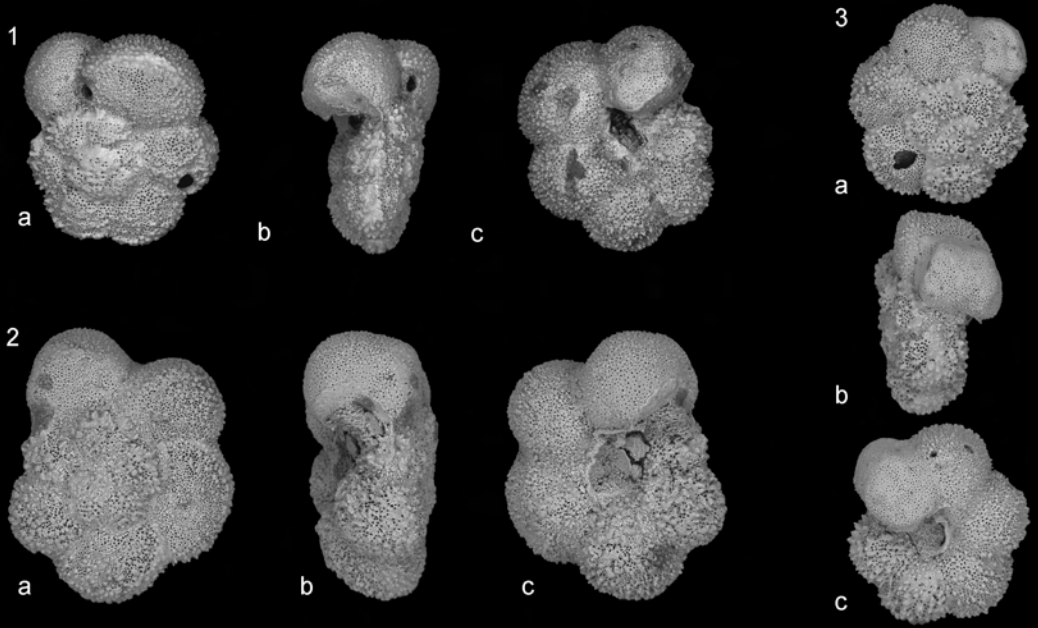
1
a
b
c
2
a
b
c
3
a
b
c
100 µm

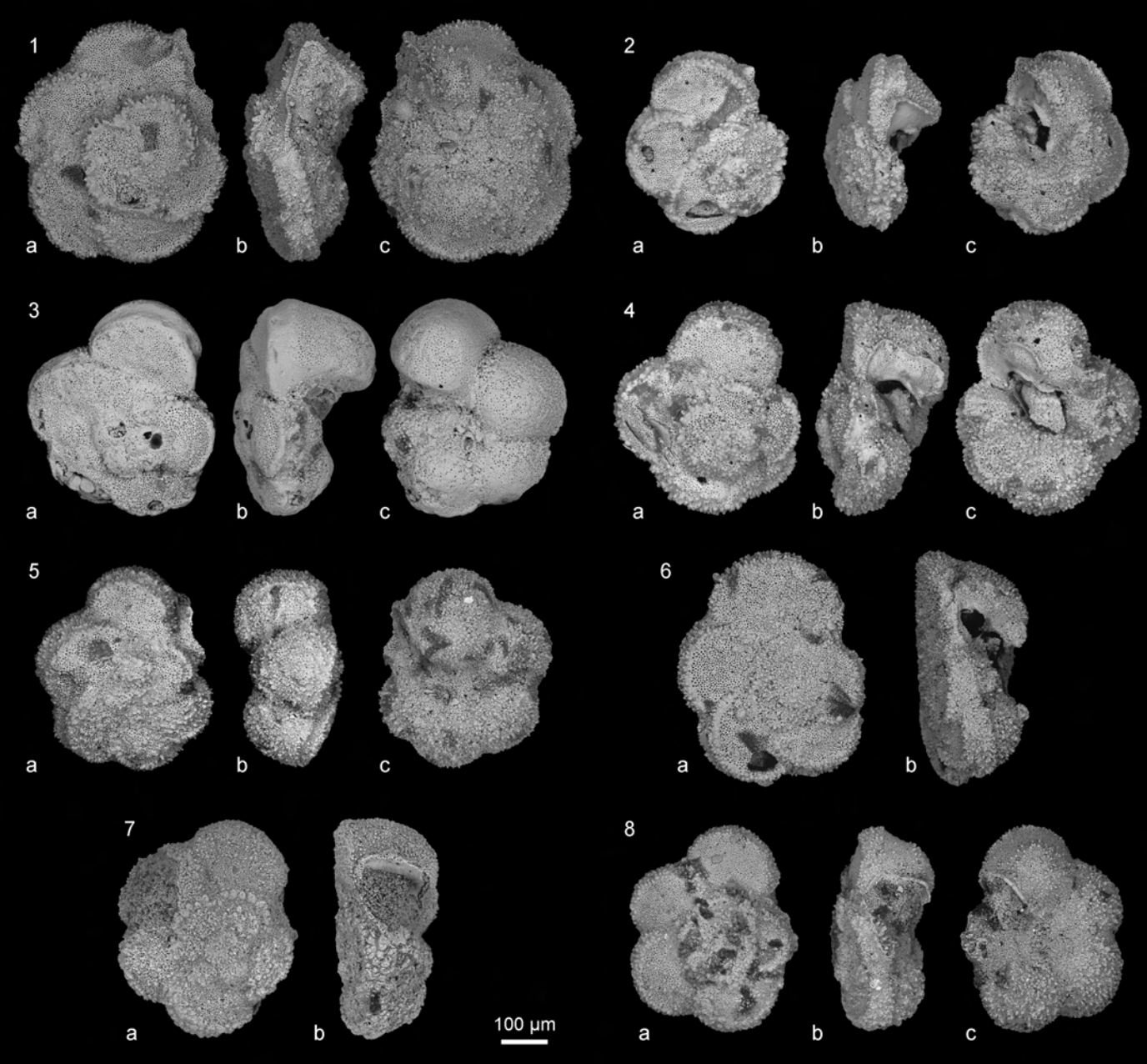
1
a
b
c
2
a
b
c
3
a
b
c
4
a
b
c
5
a
b
c
6
a
b
7
a
b
100 µm
8
a
b
c

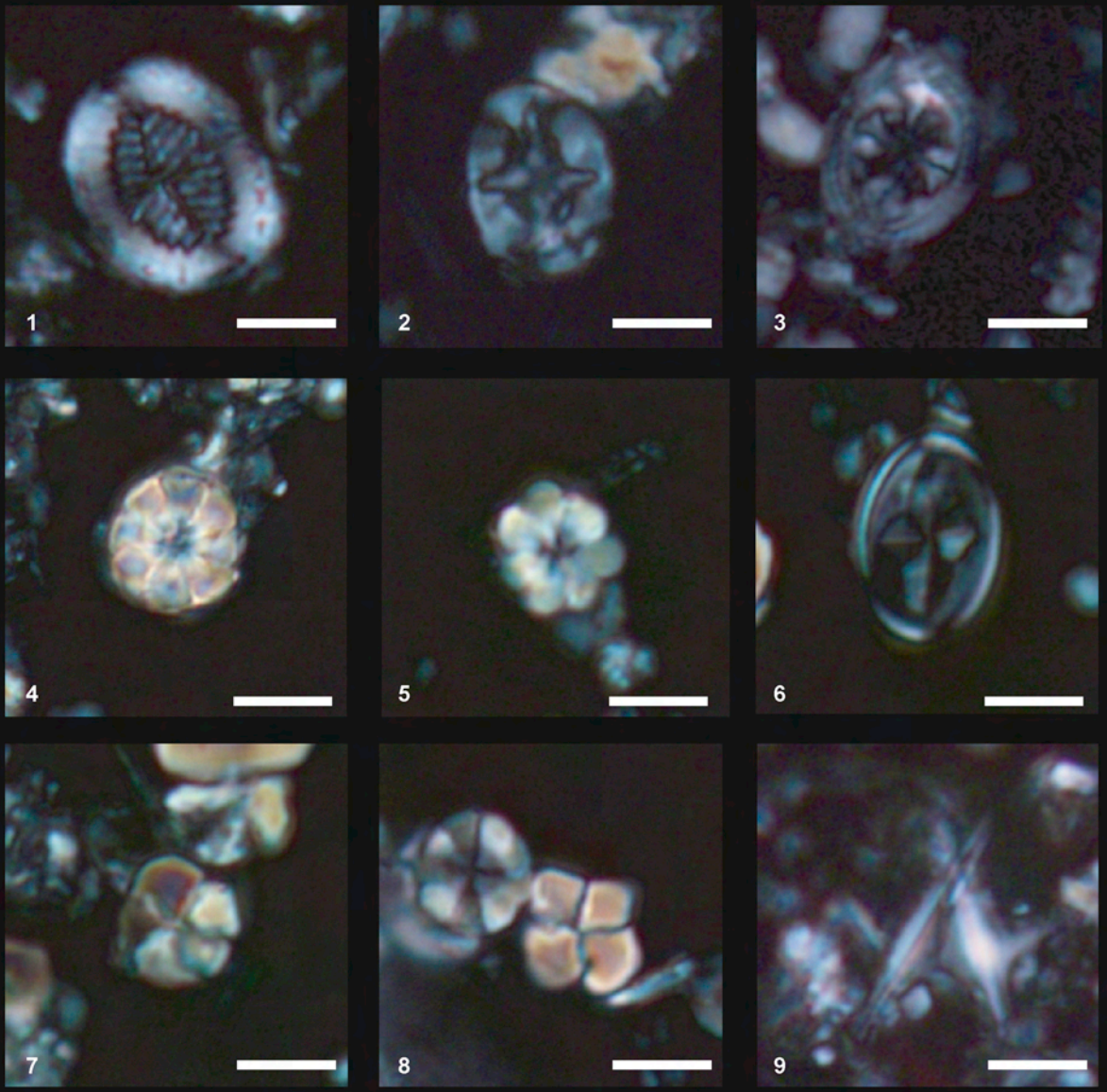
1
2
3
4
5
6
7
8
9

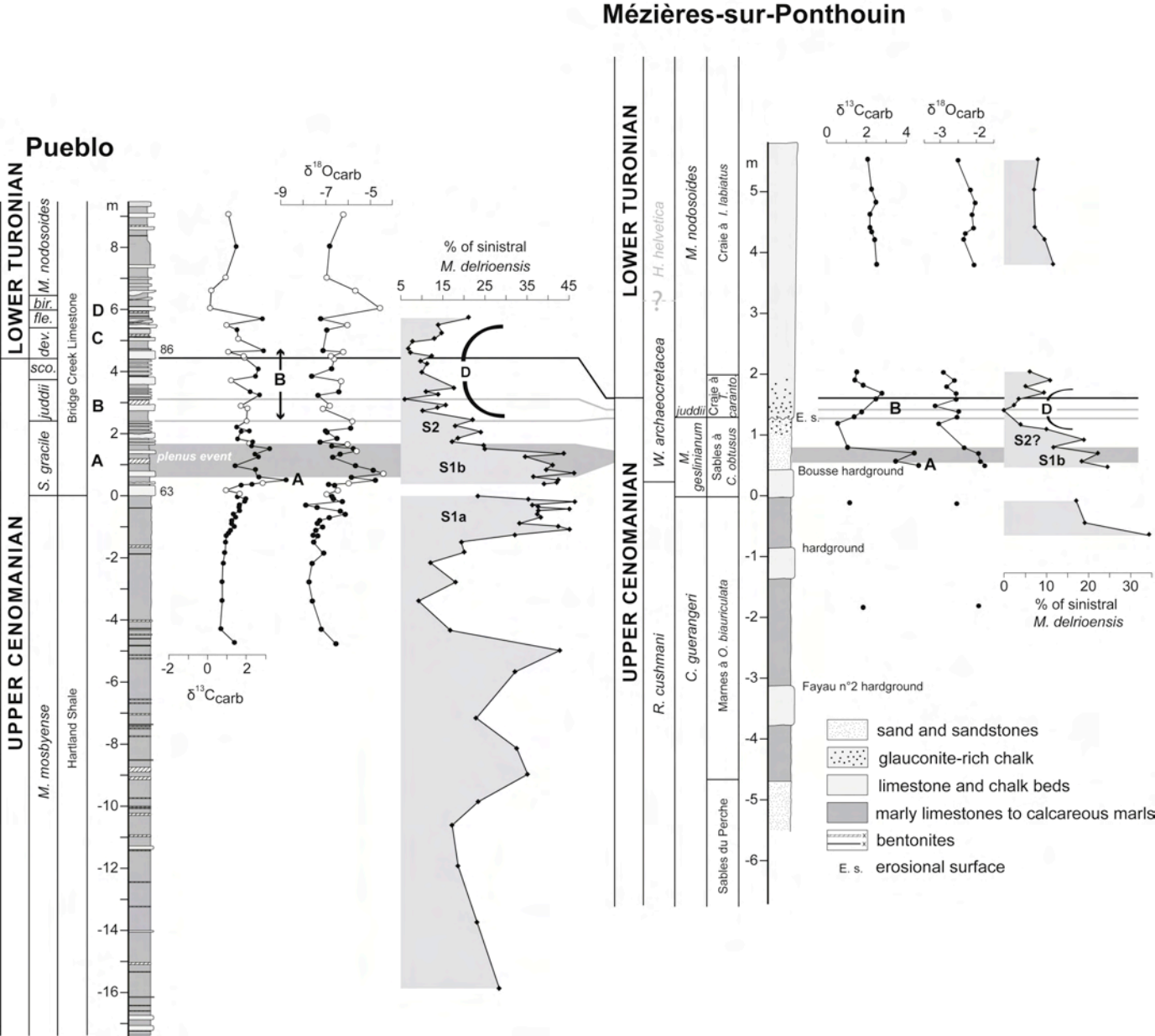
Pueblo
Mézières-sur-Ponthouin
LOWER TURONIAN
UPPER CENOMANIAN
M. nodosoides
bir.
fle.
dev.
sco.
juddii
S. gracile
M. mosbyense
Bridge Creek Limestone
Hartland Shale
δ18Ocarb
δ13Ccarb
% of sinistral
M. delrioensis
plenus event
A
B
D
S1a
S1b
S2
86
63
H. helvetica
R. cushmani
W. archaeocretacea
C. guerangeri
M. geslinianum
Craie à I. labiatus
Craie à C. carantonensis
Sables à C. obtusus
Marnes à O. biauriculata
Sables du Perche
Bousse hardground
hardground
Fayau n°2 hardground
S2?
E. s.
sand and sandstones
glauconite-rich chalk
limestone and chalk beds
marly limestones to calcareous marls
bentonites
erosional surface

Mézières-sur-Ponthouin